Published in final edited form as:

Biol Psychiatry. 2011 January 1; 69(1): 80–89. doi:10.1016/j.biopsych.2010.08.022.

Disrupted Axonal Fiber Connectivity in Schizophrenia

Andrew Zalesky, **Alex Fornito**, **Marc L. Seal**, **Luca Cocchi**, **Carl-Fredrik Westin**, **Edward T. Bullmore**, **Gary F. Egan**, and **Christos Pantelis**

Melbourne Neuropsychiatry Centre (AZ, AF, MLS, LC, CP); Florey Neuroscience Institutes (GFE, CP); Centre for Neuroscience (GFE), The University of Melbourne, Melbourne, Australia; Behavioural and Clinical Neuroscience Institute (AF, ETB), University of Cambridge, Cambridge, United Kingdom; and the Department of Radiology (C-FW), Brigham and Women's Hospital, Harvard Medical School, Boston, Massachusetts

Abstract

Background—Schizophrenia is believed to result from abnormal functional integration of neural processes thought to arise from aberrant brain connectivity. However, evidence for anatomical dysconnectivity has been equivocal, and few studies have examined axonal fiber connectivity in schizophrenia at the level of whole-brain networks.

Methods—Cortico-cortical anatomical connectivity at the scale of axonal fiber bundles was modeled as a network. Eighty-two network nodes demarcated functionally specific cortical regions. Sixty-four direction diffusion tensor-imaging coupled with whole-brain tractography was performed to map the architecture via which network nodes were interconnected in each of 74 patients with schizophrenia and 32 age- and gender-matched control subjects. Testing was performed to identify pairs of nodes between which connectivity was impaired in the patient group. The connectional architecture of patients was tested for changes in five network attributes: nodal degree, small-worldness, efficiency, path length, and clustering.

Results—Impaired connectivity in the patient group was found to involve a distributed network of nodes comprising medial frontal, parietal/occipital, and the left temporal lobe. Although small-world attributes were conserved in schizophrenia, the cortex was interconnected more sparsely and up to 20% less efficiently in patients. Intellectual performance was found to be associated with brain efficiency in control subjects but not in patients.

Conclusions—This study presents evidence of widespread dysconnectivity in white-matter connectional architecture in a large sample of patients with schizophrenia. When considered from the perspective of recent evidence for impaired synaptic plasticity, this study points to a multifaceted pathophysiology in schizophrenia encompassing axonal as well as putative synaptic mechanisms.

Address correspondence to Andrew Zalesky, Ph.D., The University of Melbourne and Melbourne Health, Melbourne Neuropsychiatry Centre, Level 3, Alan Gilbert Building, 161 Barry Street, Melbourne, Victoria VIC, Australia; ; Email: azalesky@unimelb.edu.au

The author EB is a half-time employee of GlaxoSmithKline.

All other authors reported no biomedical financial interests or potential conflicts of interest.

Supplementary material cited in this article is available online.

Keywords

Axonal connectivity; diffusion tensor imaging; network; schizophrenia; tractography; white-matter

Abnormal brain function in schizophrenia involves a distributed network of spatially separated but functionally related brain structures, including the frontal, temporal and parietal cortices, the basal ganglia, cerebellum, hippocampus, and thalamus (1). Studies modeling the brain as a network (2–5), investigations of the default-mode network in patients with schizophrenia (6–8), together with functional neuroimaging, electrophysiological studies, and theoretical neurobiology (9–20) further suggest that abnormal function in these brain structures might be coupled to disturbances within the functional circuits via which they interact. Current theories therefore posit that the cognitive and behavioral disturbances of schizophrenia are an expression of the brain's inability to properly integrate neural processes segregated across distributed regions, a state which has been termed functional dysconnectivity (18,21).

A shortcoming of functional neuroimaging and electrophysiological studies is that they cannot determine whether functional dysconnectivity stems from aberrant axonal connectivity or abnormal neuronal function within the cortical regions interconnected by a functional circuit. The former refers to axonal pathophysiologies like demyelinative processes and diminished oligodendrocyte function (22,23) as well as the possible "miswiring" of axonal fiber bundles during brain maturation, whereas the latter specifically refers to aberrant synaptic transmission and plasticity (13,18,24,35).

The former can be readily assessed with modern, noninvasive imaging techniques; namely, diffusion-weighted imaging (26) and magnetization transfer imaging (27). However, findings yielded by the application of these techniques to schizophrenia have been equivocal, with a recent meta-analysis indicating that, for any region where a positive finding was reported, at least as many studies failed to find one (1,28,29). This has led some theorists to posit that white-matter connectional architecture might be relatively preserved in schizophrenia, and the primary pathophysiology might lie in impaired synaptic plasticity (18,21,25,30).

One difficulty with studies in this field is that most of them have not directly investigated axonal connectivity per se. Instead, regions have been searched for which myelin, axonal, or other pathophysiological abnormalities are suspected, with the assumption that axonal fibers traversing the vicinity of these regions are impaired, thus suggesting a "dysconnection" between the gray-matter regions that they interconnect (31).

The principal aim of this study was to test whether white-matter connectional architecture demonstrates dysconnectivity in schizophrenia at a macroscale (i.e., at the scale of axonal fiber bundles) by mapping a network model of cortico-cortical connectivity. In particular, diffusion-weighted imaging followed by whole-brain tractography was performed to derive a network (graph) model of macroscale cortico-cortical connectivity for each of 74 patients with chronic schizophrenia and 32 control subjects. Each network node encapsulated a distinct gray-matter region, and pairs of nodes were linked if they were interconnected via

an axonal fiber (3,32–38). A network-based statistic (NBS) (Methods and Materials) was then used to identify impaired network connections in the patient group. Attributes (39) of the resulting network models were also investigated, enabling determination of whether disordered network organization was evident in schizophrenia. With these techniques, we sought to test the hypothesis that disturbed connectivity in schizophrenia is not exclusive to abnormal synaptic transmission and plasticity but also involves altered axonal connectivity as a determinant.

Methods and Materials

Sample Characteristics

Seventy-four patients with schizophrenia were recruited as part of the Australian Schizophrenia Research Bank (http://www.schizophreniaresearch.org.au). The study was approved by an independent ethics committee (Melbourne Health Research Ethics Committee, 2006: 061), and all participants were able to provide informed consent. A diagnosis of schizophrenia was confirmed with the diagnostic interview for psychoses (40). Thirty-two healthy control subjects, statistically matched ($\alpha = .05$) for average age, gender, and handedness were also recruited from similar geographic and demographic regions [age of patients: 38 ± 11 years, age of control subjects: 33 ± 13 years, $t(49.9) = 1.9$, $p = .06$; gender of patients: 47 men, gender of control subjects: 15 men, $\chi^2(1) = 2.5$, $p = .1$; handedness of patients: 62 right, handedness of control subjects: 26 right, $\chi^2(1) = 1.0$, $p = .4$].

The patient sample demonstrated a lower premorbid intelligence quotient (IQ), estimated with the Wechsler test of adult reading (41), and fewer years of education (IQ of patients: 102 ± 13, IQ of control subjects: 110 ± 9, $p < .01$; education of patients: 13 ± 13 years, education of control subjects: 16 ± 3 years, $p < .01$). Other characteristics of the patient sample were age of illness onset (23 ± .3 years) and global assessment of functioning (GAF) score (61% ± 11%); 90% of patients were on a course of antipsychotic medication, predominantly olanzapine or quetiapine. Participants were excluded if they had: a history of organic brain disorder; were younger than 16 or older than 65 years; had serious brain injury resulting in posttraumatic amnesia for more than 24 h; or had full-scale IQ < 70, movement disorder, or a current diagnosis of drug or alcohol dependence. Furthermore, control participants were excluded if they had a relative with a history of psychosis or Bipolar I Disorder or a personal history of any mental illness for which they had been hospitalized or received treatment. Participants were not excluded if they had a concurrent non-neurological or nonpsychiatric diagnosis. Participants were recruited from the community through television, newspaper, and radio advertising. No incidental findings (including white-matter hyperintensities) were noted by the radiologist in any of the structural magnetic resonance imaging scans acquired in each subject.

Acquisition and Preprocessing of Magnetic Resonance Imaging Data

A series of diffusion-weighted magnetic resonance images of brain anatomy were acquired in each subject with a Siemens Avanto 1.5-Tesla system (Siemens, Erlangen, Germany)

located at the Royal Children's Hospital, Melbourne, Australia (see Supplement 1 for acquisition parameters).

In brief, the overall preprocessing pipeline comprised the following steps: rigid-body registration of diffusion-weighted volumes to baseline T_2-weighted volume (to correct for slight head motion); stripping of skull and other noncerebral material from T_2-weighted volume; tissue classification of gray-matter, white-matter, and cerebrospinal fluid; fitting and eigen-decomposition of diffusion tensor with weighted linear least squares (42); computation of fractional anisotropy (FA) volume (43); and nonlinear normalization of FA volume to Montreal Neurological Institute space with the FMRIB58 FA image (http://www.fmrib.ox.ac.uk/fsl/) as the target. This preprocessing pipeline was repeated for each subject identically. Rigid-body registration, skull stripping, and nonlinear warping was performed with FSL software (http://www.fmrib.ox.ac.uk/fsl/).

Fiber Tract Network Model

Tractography (44–47) was performed in each subject to generate three-dimensional curves characterizing neural fiber tract connectivity. Tens of thousands of such curves, or streamlines, were generated to etch out all major white-matter tracts (34–36,38). Details of the tractography algorithm are presented in Supplement 1. Tractographic maps are shown in Figure 1 for the patient and control group.

Corticocortical fiber tract connectivity was modeled as a network, or graph, comprising a total of 82 nodes. Each node encapsulated a distinct gray-matter region, and pairs of nodes were joined by a link if they were interconnected via a sufficient number of streamlines (see Supplement 1 for details). Note that this kind of graph modeling of whole-brain connectivity derived from diffusion-weighted imaging has been previously demonstrated in healthy control subjects (32–38,48–50). Corresponding graph models of anatomical connectivity derived from cortical thickness and volumetric measurements have been studied in patients with schizophrenia (2), Alzheimer's disease (51), and multiple sclerosis (52).

Network Organization

To characterize white-matter connectional architecture, five key measures describing specific attributes of network organization were considered: nodal degree, efficiency, path length, clustering coefficient, and small-worldness (53). In brief, the *degree* of a node is the total number of connections it forms with other nodes of the network, the *path length* between two nodes is the minimum number of links that must be traversed to establish a connection, *efficiency* is the inverse of path length and is associated with how well a network supports parallel information transfer, *clustering* is a measure of the efficiency of local information transfer between neighboring nodes, and finally, a network is said to be small-world if it jointly offers long-range and local efficiency (i.e., efficient cortical integration as well as segregation). The extent to which a network is small-world was quantified with the σ-ratio. These five measures are discussed in detail in Supplement 1.

Between-group differences in each measure were investigated for a range of binarizing thresholds. A binarizing threshold of T indicates that links were only modeled between pairs of nodes interconnected by more than T streamlines.

The significance of any difference was determined with permutation testing (54) with randomized groupings of control subjects and patients. A one-tailed test of the null hypothesis was performed with the empirical null distribution.

Spearman's rank correlation was computed to assess the significance of any linear associations between variables describing the sample characteristics (i.e., age, intelligence quotient, years of education and GAF score) and measures of network organization (i.e., network efficiency, path length, clustering coefficient, σ-ratio and nodal degree).

While both groups were statistically matched for age, the patient group was on average 5 years older. Therefore, to investigate any potential age-related effects, the entire analysis was repeated with age included as a nuisance linear covariate.

Impaired Connections

Statistical testing was performed to identify any pairs of nodes (cortical regions) that were connected in control subjects but demonstrated impaired connectivity in patients. The connectivity between a pair of nodes was quantified by the total number of streamlines that interconnected them. Furthermore, a particular connection was said to be impaired if it comprised significantly fewer streamlines in patients than in control subjects (see Discussion for suggestions on the pathophysiological significance of a reduced streamline count).

Statistical testing was performed on the subset of all pairs of nodes that were connected on average by at least K_{avg} streamlines in the control group. This constraint ensured a connection was not assumed between a pair of nodes that happened to be connected as a matter of chance by one or two potentially spurious streamlines.

The null hypothesis of equal connectivity between control subjects and patients (i.e., equal streamline count) was considered for all node pairs satisfying the K_{avg} threshold. A one-tailed p value was calculated independently for each hypothesis with permutation testing (5000 permutations), as described in the preceding text. The false discovery rate (FDR) was used to correct for multiple comparisons (55).

Impaired Networks

The NBS (56) was used to identify and ascribe significance to any connected subnetworks evident in the set of impaired links found in the Impaired Connections section of this text. The NBS is described in Supplement 1. The NBS was used with the following parameter settings: $K_{avg} = 2$, the primary threshold for each link-based t statistic was set to 1.5, and only cortico-cortical streamlines exceeding 20 mm in length were used to generate the connectivity matrix for each subject. Figure 1 shows an overview of the complete methodology used in this study.

Results

Anomalous Network Organization

Anomalous network organization was investigated for graph binarizing thresholds in the range $T = 0,1,\ldots 8$. Thresholds exceeding $T = 8$ resulted in highly fragmented graphs and were therefore not considered.

Average nodal degree and network efficiency were significantly reduced in patients for all thresholds considered (Figure 2). The maximum decrease in nodal degree was 10% and found at $T = 8$, whereas the maximum difference in efficiency was 22% and also found at $T = 8$.

Note that efficiency and nodal degree are not independent measures; graphs of higher degree typically offer greater efficiency, simply because they comprise more links. Therefore, a likely contributing factor to the reduction in efficiency found in patients was the fact that their cortices were more sparsely interconnected (i.e., lower nodal degree).

To attribute the observed change in global efficiency to particular cortical regions, regional network efficiency (57,58) was calculated individually for each node. Although several parietal, occipital, and frontal nodes were found to show a trend toward diminished efficiency, no such difference survived FDR correction.

Both patients and control subjects were found to demonstrate small-world topologies. In particular, both groups demonstrated clustering coefficients that were considerably larger than degree-matched random graphs (>8× greater for $T = 4$) (Figure 2), whereas path lengths were only marginally longer (<1.5 × longer for $T = 4$). Therefore, the optimal balance between local specialization and global integration (59) arising from the small-world nature of anatomical connectivity seems to be conserved in schizophrenia.

A trend toward increased path length, clustering, and σ-ratio was found in patients, but these differences were not significant for most thresholds (Figure 2).

A strong linear association was found in the control group between intelligence quotient and three key attributes of network organization: global efficiency, path length, and clustering coefficient (Figure 3). No such associations were found in the patient group (Supplement 1).

Significant associations with age, years of education, and GAF score were not found. The significance of all the reported results remained unchanged when the analysis was repeated with age included as a nuisance linear covariate.

Impaired Connections

Having found anomalous network organization at a global level, the next step was to introduce localizing power and attempt to pinpoint particular cortical pairs that were abnormally connected in patients. Impaired connectivity was tested in all links satisfying a threshold of $K_{avg} = 4$, meaning that, for a node pair to be tested, it had to be connected on average by at least four streamlines in the control group.

For an FDR of 5%, three node pairs showed impaired connectivity (i.e., reduced streamline count) in patients: 1) right angular and right middle temporal; 2) right superior frontal and left superior frontal; and 3) left inferior frontal triangularis and left insula.

An additional two pairs showed a trend toward impaired connectivity (i.e., FDR < 10%): 1) left cuneus and right superior occipital; and 2) left cuneus and right cuneus.

The anatomical name by which each node is labeled was taken directly from the Anatomical Automatic Labeling Atlas (60). Streamlines interconnecting each of these five node pairs were visualized to gain insight into the trajectory and morphology of the fiber tracts they represented (Figure 4).

An increased streamline count in patients was also tested but not found significant for any node pairs. The results presented in this section were stable to variations in the threshold K_{avg} not exceeding ±1.5.

Impaired Network

The NBS was used to identify any connected networks that were evident in control subjects but not in patients. A single network was found to be significantly impaired in patients ($p < .05$, corrected). The network interconnected medial frontal regions and several nodes comprising the parietal/occipital lobes. A total of 14 nodes (of 82) and 15 links were involved. Streamlines interconnecting this network were visualized as three-dimensional curves, and the volume encapsulated by each node was rendered atop the streamline trajectories (Figure 5). A schematic representation of the network was also depicted (Figure 5). The significance of the network remained unchanged when subject age was included as a nuisance linear covariate for each link-based test. The sensitivity of the results were found to be robust to alternative NBS parameter settings (Supplement 1).

Discussion

The present study found evidence of dysconnection in white-matter connectional architecture in a large sample of patients with schizophrenia. When considered from the perspective of mounting evidence for impaired synaptic plasticity (13,18,24,25), this result suggests that functional dysconnectivity in schizophrenia might be the result of a multifaceted pathophysiology involving both axonal in addition to putative synaptic mechanisms. Indeed, both mechanisms can coexist (21).

Impaired connectivity in schizophrenia was found to involve three regionally distinct groups of nodes: medial frontal, parietal/occipital, and left temporal. In patients, the frontal group was less well-connected to the parietal/occipital group via the cingulum bundle and left posterior cingulate, whereas multiple transcallosal pathways interconnecting contralateral nodes within the frontal and parietal/occipital groups also demonstrated disruption. Both the cingulum (61–64) and the corpus callosum (65–69) have been implicated in several previous voxelwise and morphological investigations of schizophrenia. Cingulate dysfunction is widely implicated in the pathophysiology of schizophrenia (70–73), and this study provides

new evidence suggesting that its connections with an extended network of cortical regions is altered in the disorder.

The nodes found to demonstrate the greatest number of disruptions were the right superior occipital node (degree of 2 in Figure 5, degree of 5 in Figure S3 in Supplement 1), left middle occipital node (degree 3 and 4), and the left precuneus (degree 5 and 2). It is important to note that the null hypothesis cannot be rejected for each of these nodes individually but only at the level of the subnetwork they comprise. Other implicated nodes included the antero- and postero-medial components of the so-called default mode network, which have been identified as important connectivity hubs in functional brain networks (74,75). These findings also converge with structural imaging evidence suggesting these medial components of the default mode network are among the most commonly reported regions showing gray-matter changes in schizophrenia (31,72,76,77).

In addition, Figure 4 implicated connections originating from the left insula, superior frontal gyrus bilaterally, and a midtemporal region; however, these connections were not detected by the NBS (Figure 5). Note that the NBS does not have the ability to detect impaired connections that exist in isolation (i.e., connections that do not form an interconnected subnetwork)—and hence, the likely reason for some of the impaired connections identified in Figure 4 not featuring in Figure 5 and Figure S3 in Supplement 1.

It should be noted that some regions, such as the medial and lateral temporal areas, were not identified as showing strong connectivity differences in our study, despite often showing volumetric reductions in patients. This discrepancy might reflect the fact that our analysis is indexing a distinct aspect of neuropathology—namely, connectivity as opposed to volume.

By localizing connectivity impairments in schizophrenia to a specific subset of cortical regions, the present study provides fresh evidence for the macro-circuit theory of schizophrenia (1,78), which posits only specific white-matter fibers are disrupted in schizophrenia, either as a secondary effect owing to neuronal dysfunction in the gray-matter regions they interconnect or as a primary pathophysiology in schizophrenia. Although regional white-matter differences reported in previous studies also support this theory, these studies have not been able to model connectivity disturbances across the entire brain. In contrast, our approach represents a first step toward a whole-brain description of connectivity disturbances in schizophrenia. More specifically, our findings point to a network of anterior and posterior medial regions as a key macro-circuit affected in schizophrenia. Interestingly, this network bears close resemblance to a previously identified connectivity core in human cortical networks (35), which might support efficient functional dynamics (48).

Intellectual performance in the control group was strongly associated with network efficiency, path length, and clustering, which is consistent with previous studies (3,79) and supports the notion that specific properties of brain network organization have functional importance. No such associations were evident in patients.

Pathophysiological Significance

In this study, the differences found in patients can all have their origins traced back to a reduction in the total number of streamlines interconnecting particular pairs of gray-matter nodes. It is currently not understood whether a reduction in the number of streamlines supporting a fiber tract can be ascribed to demyelinative processes or to a reduction in the number, density, or coherence of axon fibers. The speed at which information can be transferred between a pair of cortical regions connected via an impaired fiber tract is possibly diminished; in particular, a reduction in axonal number or density might imply fewer nerve pulses are transferred, hence less information is carried (1), whereas demyelination results in a slowdown of the conduction velocity of nerve pulses (80), thereby also reducing information transfer.

Volumetric reductions in white-matter and ventricular increases have been reported in some structural studies in schizophrenia (81). Volumetric changes were a potential confound in this study, because a separate streamline was initialized from every voxel classified as white-matter. Therefore, a significant volumetric white-matter reduction might have resulted in a systematic reduction in the number of streamlines initialized in patients. However, a significant difference between groups with respect to the total number of streamlines (i.e., inclusive of cortico-cortical, corticospinal, subcortical, and cerebellum and not length thresholded) was not evident. Note that streamlines were significantly longer in control subjects (length in patients: 4.7 ± .3 cm, length in control subjects: 4.9 ± .3 cm, $t = 2.7$, $p = .009$), and the total number of streamlines exceeding 20 mm in length was also significantly greater in control subjects (total patients: 15,380 ± 3651; total control subjects: 17,230 ± 3251, $t = 2.4$, $p = .02$). Furthermore, in a supplementary analysis, it was found that the number of voxels classified as white-matter was not significantly different between both groups (Figure S1 in Supplement 1). Although these findings cannot rule out localized atrophies, they suggest that global differences in white-matter volume were unlikely to be the predominant factor underlying the effects reported in this study. Any potential differences in gray-matter volume are unlikely to be the source of these effects, because tractography was explicitly constrained to white-matter and all connectivity maps were normalized to a standard space where a common gray-matter parcellation was used.

Methodological Considerations

Previous studies have searched for regions at which myelin, axonal, or other pathophysiological changes are suspected, with single-valued measures like FA. If abnormalities are detected, the assumption is that any fiber tracts traversing or encompassed by these anomalous regions are damaged, thus suggesting a dysconnection between the gray-matter regions that they interconnect. However, due to the diffuse nature of localized findings, it can be difficult to implicate specific fiber bundles affected by a localized change in white-matter. For example, as Kanaan *et al.* (28) pointed out, the study of Ardekani *et al.* (82) was only able to report anisotropy reductions “in the vicinity” of the cingulum, because the localized difference found also implicated the corpus callosum and other distinct fasciculi. Although recent studies (83–85) have delineated fiber tracts of interest with tractography and then parameterized anisotropy along the delineated tract, these studies are disadvantaged by the need for tract-specific hypotheses.

In the present study, whole-brain tractography was performed to derive a cortico-cortical network model of white-matter connectional architecture. Although this approach is more sensitive to network disruptions, the results are contingent on the accuracy of the tractography algorithm.

The fiber assignment by continuous tracking (FACT) streamline tracking algorithm (86) was used in this study. The FACT algorithm is simple, computationally inexpensive, and has been demonstrated to yield robust tractographic maps. However, streamline tracking algorithms in general are known to have difficulty in following long distance fibers, either due to partial volume effects, a poor fit of the diffusion tensor, or simply due to noise (37). Therefore, the ability to resolve long association fibers, such as the arcuate fasciculus, was limited in this study. Although advanced tractographic algorithms (e.g., 36,37,87–90) alleviate some of the limitations inherent to streamline tracking, they might not be computationally feasible for studies involving hundreds of subjects.

Furthermore, complex tract geometries (i.e., crossing fibers) resulting in a non-Gaussian diffusion profile were not modeled, which could have potentially resulted in a failure to detect some connections. If crossing fibers were modeled, tractographic maps demonstrating a more extensive lateral and interhemispheric connectivity pattern could have been expected (38). Moreover, although the cortical nodes between which connectivity was impaired were identified, due to limitations of the tractography algorithm and because the crossing fibers were not modeled, it might be difficult to pinpoint the precise axonal bundles responsible for the loss of connectivity between each cortical pair identified.

Finally, the findings reported in this study might potentially be interpreted as effects arising from the significantly lower IQ of the patient group; however, disassociating low IQ from the disorder per se is generally difficult, given the pervasive cognitive difficulties shown by most patients (91). Furthermore, although the influence of antipsychotic medication and duration of illness on white-matter morphology cannot be ruled out in this study due to the nature of the patient sample, recent studies (92) suggest no white-matter differences between chronically and briefly medicated patients and no correlation with illness duration. Finally, although white-matter hyperintensities were not noted by the radiologist, the presence of subtle anomalies was possible in the individuals over the age of 50 years (93,94), which might have affected connectivity measurements. Note that 11 patients and 4 control subjects were over the age of 50 years, whereas 1 patient and 1 control subject were over the age of 60 years. Future work will investigate any potential concordance with impaired functional connectivity, an avenue that has received recent attention in Honey *et al.* (48) and Skudlarski *et al.* (95).

Supplementary Material

Refer to Web version on PubMed Central for supplementary material.

Acknowledgments

This study was supported by the Australian Schizophrenia Research Bank, which is supported by the National Health and Medical Research Council (NHMRC) of Australia, the Pratt Foundation, Ramsay Health Care, the

Viertel Charitable Foundation, and the Schizophrenia Research Institute. The computing resources used to undertake this study were provided by the Florey Neuroscience Institutes and the Department of Electrical and Electronic Engineering at the University of Melbourne. Software development was supported by a Human Brain Project grant from the National Institute of Biomedical Imaging and Bioengineering and the National Institute of Mental Health. Graph measures reported in this article were computed with the MatlabBGL package written by D. Gleich. The author AZ is supported by the Australian Research Council (ID: DP0986320). The author AF is supported by an NHMRC CJ Martin Fellowship (ID: 454797). The author MLS is sup-ported by a Ronald Phillip Griffith Fellowship. The author LC is supported by the Swiss Academy of Medical Science and the Swiss National Science Foundation (ID: PASMP3 129357/1). The author CP is supported by an NHMRC Senior Principal Research Fellowship (ID: 628386). The author CFW is supported by National Institutes of Health (NIH) grants: Novel DT-MRI Analyses of White Matter in Schizophrenia (ID: NIH R01MH074794) and Neuroimage Analysis Center (ID: NIH P41RR013218).

References

1. Konrad A, Winterer G. Disturbed structural connectivity in schizophrenia–primary factor in pathology or epiphenomenon? Schizophr Bull. 2008; 34:72–92. [PubMed: 17485733]
2. Bassett DS, Bullmore E, Verchinski BA, Mattay VS, Weinberger DR, Meyer-Lindenberg A. Hierarchical organization of human cortical networks in health and schizophrenia. J Neurosci. 2008; 28:9239–9248. [PubMed: 18784304]
3. Li Y, Liu Y, Li J, Qin W, Kuncheng L, Yu C, Jiang T. Brain anatomical network and intelligence. PLoS Comput Biol. 2009; 5:e1000395. [PubMed: 19492086]
4. Liu Y, Liang M, Zhou Y, He Y, Hao Y, Song M, et al. Disrupted small-world networks in schizophrenia. Brain. 2008; 131:945–961. [PubMed: 18299296]
5. Rubinov M, Knock SA, Stam CJ, Micheloyannis S, Harris AWF, Williams LM, Breakspear M. Small-world properties of nonlinear brain activity in schizophrenia. Hum Brain Mapp. 2009; 30:403–416. [PubMed: 18072237]
6. Bluhm RL, Miller J, Lanius RA, Osuch EA, Boksman K, Neufeld RW, et al. Spontaneous low-frequency fluctuations in the BOLD signal in schizophrenic patients: anomalies in the default network. Schizophr Bull. 2007; 33:1004–1012. [PubMed: 17556752]
7. Camchong J, Macdonald AW, Bell C, Mueller BA, Lim KO. Altered functional and anatomical connectivity in schizophrenia [published online ahead of print November 17]. Schizophr Bull. 2009; doi: 10.1093/schbul/sbp131
8. Garrity AG, Pearlson GD, McKiernan K, Lloyd D, Kiehl KA, Calhoun VD. Aberrant “default mode” functional connectivity in schizophrenia. Am J Psychiatry. 2007; 164:450–457. [PubMed: 17329470]
9. Andreasen NC, Paradiso S, O’Leary DS. “Cognitive dysmetria” as an integrative theory of schizophrenia: A dysfunction in cortical-subcortical-cerebellar circuitry? Schizophr Bull. 1998; 24:203–218. [PubMed: 9613621]
10. Bullmore ET, Frangou S, Murray RM. The dysplastic net hypothesis: An integration of developmental and disconnectivity theories of schizophrenia. Schizophr Res. 1997; 28:143–156. [PubMed: 9468349]
11. Fletcher P, McKenna PJ, Friston KJ, Frith CD, Dolan RJ. Abnormal cingulate modulation of fronto-temporal connectivity in schizophrenia. Neuroimage. 1999; 9:337–342. [PubMed: 10075903]
12. Friston KJ, Frith CD. Schizophrenia: A disconnection syndrome? Clin Neurosci. 1995; 3:89–97. [PubMed: 7583624]
13. Friston KJ. The disconnection hypothesis. Schizophr Res. 1998; 30:115–125. [PubMed: 9549774]
14. Friston KJ. Dysfunctional connectivity in schizophrenia. World Psychiatry. 2002; 1:66–71. [PubMed: 16946855]
15. Hoffman RE, Buchsbaum MS, Escobar MD, Makuch RW, Nuechterlein KH, Guich SM. EEG coherence of prefrontal areas in normal and schizophrenic males during perceptual activation. J Neuropsychiatr Clin Neurosci. 1991; 3:169–175.
16. Meyer-Lindenberg A, Poline JP, Kohn PD, Holt MS, Egan MF, Weinberger DR, Berman KF. Evidence for abnormal cortical functional connectivity during working memory in schizophrenia. Am J Psychiatry. 2001; 158:1809–1817. [PubMed: 11691686]

17. Pantelis C, Barnes TR, Nelson HE. Is the concept of frontal-subcortical dementia relevant to schizophrenia? Br J Psychiatry. 1992; 160:442–460. [PubMed: 1349250]
18. Stephan KE, Baldeweg T, Friston KJ. Synaptic plasticity and dysconnection in schizophrenia. Biol Psychiatry. 2006; 59:929–939. [PubMed: 16427028]
19. Weinberger DR. A connectionist approach to the prefrontal cortex. J Neuropsychiatr Clin Neurosci. 1993; 5:241–253.
20. Winterer G, Coppola R, Egan MF, Goldberg TE, Weinberger DR. Functional and effective frontotemporal connectivity and genetic risk for schizophrenia. Biol Psychiatry. 2003; 54:1181–1192. [PubMed: 14643085]
21. Stephan KE, Friston KJ, Frith CD. Dysconnection in schizophrenia: From abnormal synaptic plasticity to failures of self-monitoring. Schizophr Bull. 2009; 35:509–527. [PubMed: 19155345]
22. Hakak Y, Walker JR, Li C, Wong WH, Davis KL, Buxbaum JD, et al. Genome-wide expression analysis reveals dysregulation of myelination-related genes in chronic schizophrenia. Proc Natl Acad Sci U S A. 2001; 98:4746–4751. [PubMed: 11296301]
23. Uranova NA, Casanova MF, DeVaughn NM, Orlovskaya DD, Denisov DV. Ultrastructural pathology of neuronal connectivity in postmortem brains of schizophrenic patients. Schizophr Res. 1996; 22:81–83. [PubMed: 8908694]
24. Daskalakis ZJ, Christensen BK, Fitzgerald PB, Chen R. Dysfunctional and neural plasticity in patients with schizophrenia. Arch Gen Psychiatry. 2008; 65:378–385. [PubMed: 18391126]
25. McGlashan TH, Hoffman RE. Schizophrenia as a disorder of developmentally reduced synaptic connectivity. Arch Gen Psychiatry. 2000; 57:637–648. [PubMed: 10891034]
26. Basser PJ, Mattiello J, LeBihan D. Diffusion tensor MR imaging of the human brain. Radiology. 1996; 201:637–648. [PubMed: 8939209]
27. Foong J, Symms MR, Barker GJ, Maier M, Woermann FG, Miller DH, Ron MA. Neuropathological abnormalities in schizophrenia: Evidence from magnetization transfer imaging. Brain. 2001; 124:882–892. [PubMed: 11335691]
28. Kanaan RAA, Kim JS, Kaufmann WE, Pearlson GD, Barker GJ, McGuire PK. Diffusion tensor imaging in schizophrenia. Biol Psychiatry. 2005; 58:921–929. [PubMed: 16043134]
29. Kubicki M, McCarley RW, Shenton ME. Evidence for white matter abnormalities in schizophrenia. Curr Opin Psychiatry. 2005; 18:121–134. [PubMed: 16639164]
30. Feinberg I. Schizophrenia: Caused by a fault in programmed synaptic elimination during adolescence? J Psychiatr Res. 1982; 17:319–334. [PubMed: 7187776]
31. Ellison-Wright I, Glahn DC, Laird AR, Thelen SM, Bullmore E. The anatomy of first-episode and chronic schizophrenia: An anatomical likelihood estimation meta-analysis. Am J Psychiatry. 2008; 165:1015–1023. [PubMed: 18381902]
32. Gong G, He Y, Concha L, Lebel C, Gross DW, Evans AC, Beaulieu C. Mapping anatomical connectivity patterns of human cerebral cortex using in vivo diffusion tensor imaging tractography. Cereb Cortex. 2009; 9:524–536. [PubMed: 18567609]
33. Gong G, Rosa-Neto P, Carbonell F, Chen ZJ, He Y, Evans AC. Age-and gender-related differences in the cortical anatomical network. J Neurosci. 2009; 29:15684–15693. [PubMed: 20016083]
34. Hagmann P, Kurant M, Gigandet X, Thiran P, Wedeen VJ, Meuli R, Thiran J-P. Mapping human whole-brain structural networks with diffusion MRI. PLoS ONE. 2007; 2:e597. [PubMed: 17611629]
35. Hagmann P, Cammoun L, Gigandent X, Meuli R, Honey CJ, Wedeen VJ, Sporns O. Mapping the structural core of the human cerebral cortex. PLoS Biol. 2008; 6:e159. [PubMed: 18597554]
36. Iturria-Medina Y, Sotero RC, Canales-Rodríguez EJ, Alemán-Gómez Y, Melie-García L. Studying the human brain anatomical network via diffusion-weighted MRI and graph theory. Neuroimage. 2008; 40:1064–1076. [PubMed: 18272400]
37. Zalesky A, Fornito A. A DTI-derived measure of cortico-cortical connectivity. IEEE Trans Med Imaging. 2009; 28:1023–1036. [PubMed: 19150781]
38. Zalesky A, Fornito A, Harding IH, Cocchi L, Yücel M, Pantelis C, Bullmore ET. Whole-brain anatomical networks: Does the choice of nodes matter? Neuroimage. 2010; 50:970–83. [PubMed: 20035887]

39. Bullmore E, Sporns O. Complex brain networks: Graph theoretical analysis of structural and functional systems. Nat Rev Neurosci. 2009; 10:186–198. [PubMed: 19190637]
40. Castle DJ, Jablensky A, McGrath JJ, Carr V, Morgan V, Waterreus A, et al. The diagnostic interview for psychoses (DIP): Development, reliability and applications. Psychol Med. 2006; 36:69–80. [PubMed: 16194284]
41. Wechsler, D. Manual for the Wechsler Adult Intelligence Scale (WAIS-R). San Antonio, Texas: Psychological Corporation; 1981.
42. Salvador R, Pena A, Menon DK, Adrian Carpenter T, Pickard JD, Bullmore E. Formal characterization and extension of the linearized diffusion tensor model. Hum Brain Mapp. 2005; 24:144–155. [PubMed: 15468122]
43. Basser PJ. Inferring microstructural features and the physiological state of tissues from diffusion-weighted images. NMR Biomed. 1995; 8:333–344. [PubMed: 8739270]
44. Basser PJ, Pajevic S, Pierpaoli C, Duda J, Aldroubi A. In vivo fiber tractography using DT-MRI data. Magn Reson Med. 2000; 44:625–632. [PubMed: 11025519]
45. Catani M, Howard RJ, Pajevic S, Jones DK. Virtual in vivo interactive dissection of white matter fasciculi in the human brain. Neuroimage. 2002; 17:77–94. [PubMed: 12482069]
46. Catani M. Diffusion tensor magnetic resonance imaging tractography in cognitive disorders. Curr Opin Neurol. 2006; 19:599–606. [PubMed: 17102700]
47. Conturo TE, Lori NF, Cull TS, Akbudak E, Snyder AZ, Shimony JS, et al. Tracking neuronal fiber pathways in the living human brain. Proc Natl Acad Sci U S A. 1999; 96:10422–10427. [PubMed: 10468624]
48. Honey CJ, Sporns O, Cammoun L, Gigandet X, Thiran J-P, Meuli R, Hagmann P. Predicting human resting-state functional connectivity from structural connectivity. Proc Natl Acad Sci U S A. 2009; 106:2035–2040. [PubMed: 19188601]
49. Park C-H, Kim SY, Kim Y-H, Kim K. Comparison of the small-world topology between anatomical and functional connectivity in the human brain. Phys A. 2008; 387:5958–5962.
50. Skudlarski P, Jagnnathan K, Calhoun VD, Hampson M, Skudlarska BA, Pearlson G. Measuring brain connectivity: Diffusion tensor imaging validates resting state temporal correlations. Neuroimage. 2008; 43:554–561. [PubMed: 18771736]
51. He Y, Chen ZJ, Evans AC. Structural insights into aberrant topological patterns of large-scale cortical networks in Alzheimer's disease. J Neurosci. 2008; 28:5756–4766. [PubMed: 18509037]
52. He Y, Dagher A, Chen Z, Charil A, Zijdenbos A, Worsley K, Evans A. Impaired small-world efficiency in structural cortical networks in multiple sclerosis associated with white matter lesion load. Brain. 2009; 132:3366–3379. [PubMed: 19439423]
53. Rubinov M, Sporns O. Complex network measures of brain connectivity: Uses and interpretations. Neuroimage. 2010; 52:1059–1069. [PubMed: 19819337]
54. Nichols TE, Holmes AP. Nonparametric permutation tests for functional neuroimaging: A primer with examples. Hum Brain Mapp. 2001; 15:1–25. [PubMed: 11747097]
55. Genovese CR, Lazar NA, Nichols T. Thresholding of statistical maps in functional neuroimaging using the false discovery rate. Neuroimage. 2002; 15:870–878. [PubMed: 11906227]
56. Zalesky A, Fornito A, Bullmore ET. Network-based statistic: Identifying differences in brain networks. Neuroimage. 2010; 53:1197–1207. [PubMed: 20600983]
57. Achard S, Bullmore E. Efficiency and cost of economical brain functional networks. PLoS Comput Biol. 2007; 3:e17. [PubMed: 17274684]
58. Latora V, Marchiori M. Efficient behavior of small-world networks. Phys Rev Lett. 2001; 87:198–701.
59. Sporns O, Tononi G, Edelman GM. Theoretical neuroanatomy: Relating anatomical and functional connectivity in graphs and cortical connection matrices. Cereb Cortex. 2000; 10:127–141. [PubMed: 10667981]
60. Tzourio-Mazoyer N, Landeau B, Papathanassiou D, Crivello F, Etard O, Delcroix N, et al. Automated anatomical labeling of activations in SPM using a macroscopic anatomical parcellation of the MNI MRI single-subject brain. Neuroimage. 2002; 15:273–289. [PubMed: 11771995]

61. Kubicki M, Westin CF, Nestor PG, Wible CG, Frumin M, Maier SE, et al. Cingulate fasciculus integrity disruption in schizophrenia: A magnetic resonance diffusion tensor imaging study. Biol Psychiatry. 2003; 54:1171–1180. [PubMed: 14643084]
62. Seal ML, Yucel M, Fornito A, Wood SJ, Harrison BJ, Walterfang M, et al. Abnormal white matter microstructure in schizophrenia: A voxelwise analysis of axial and radial diffusivity. Schizophr Res. 2008; 101:106–110. [PubMed: 18262770]
63. Sun Z, Wang F, Cui L, Breeze J, Du X, Wang X, et al. Abnormal anterior cingulum in patients with schizophrenia: A diffusion tensor imaging study. Neuroreport. 2003; 14:1833–1836. [PubMed: 14534430]
64. Wang F, Sun Z, Cui L, Du X, Wang X, Zhang H, et al. Anterior cingulum abnormalities in male patients with schizophrenia determined through diffusion tensor imaging. Am J Psychiatry. 2004; 161:573–575. [PubMed: 14992988]
65. Cheung V, Cheung C, McAlonan GM, Deng Y, Wong JG, Yip L, et al. A diffusion tensor imaging study of structural disconnectivity in never-medicated, first-episode schizophrenia. Psychol Med. 2008; 38:877–885. [PubMed: 17949516]
66. Gasparotti R, Valsecchi P, Carletti F, Galluzzo A, Liserre R, Cesana B, Sacchetti E. Reduced fractional anisotropy of corpus callosum in first-contact, antipsychotic drug-naive patients with schizophrenia. Schizophr Res. 2009; 108:41–48. [PubMed: 19103476]
67. Kubicki M, Styner M, Bouix S, Gerig G, Markant D, Smith K, et al. Reduced interhemispheric connectivity in schizophrenia-tractography based segmentation of the corpus callosum. Schizophr Res. 2008; 106:125–131. [PubMed: 18829262]
68. Walterfang M, Yung A, Wood AG, Reutens DC, Phillips L, Wood SJ, et al. Corpus callosum shape alterations in individuals prior to the onset of psychosis. Schizophr Res. 2008; 103:1–10. [PubMed: 18562178]
69. Walterfang M, Wood AG, Reutens DC, Wood SJ, Chen J, Velakoulis D, et al. Morphology of the corpus callosum at different stages of schizophrenia: Cross-sectional study in first-episode and chronic illness. Br J Psychiatry. 2008; 192:429–434. [PubMed: 18515892]
70. Benes FM. Neurobiological investigations in cingulate cortex of schizophrenic brain. Schizophr Bull. 1993; 19:537–549. [PubMed: 8235456]
71. Fornito A, Yucel M, Dean B, Wood SJ, Pantelis C. Anatomical abnormalities of the anterior cingulate cortex in schizophrenia: Bridging the gap between neuroimaging and neuropathology. Schizophr Bull. 2009; 35:973–993. [PubMed: 18436528]
72. Glahn DC, Laird AR, Ellison-Wright I, Thelen SM, Robinson JL, Lancaster JL, et al. Meta-analysis of gray matter anomalies in schizophrenia: Application of anatomic likelihood estimation and network analysis. Biol Psychiatry. 2008; 64:774–781. [PubMed: 18486104]
73. Snitz BE, MacDonald A, Cohen JD, Cho RY, Becker T, Carter CS. Lateral and medial hypofrontality in first-episode schizophrenia: Functional activity in a medication-naive state and effects of short-term atypical antipsychotic treatment. Am J Psychiatry. 2005; 162:2322–2329. [PubMed: 16330597]
74. Buckner RL, Sepulcre J, Talukdar T, Krienen FM, Liu H, Hedden T, et al. Cortical hubs revealed by intrinsic functional connectivity: Mapping, assessment of stability, and relation to Alzheimer's disease. J Neurosci. 2009; 29:1860–1873. [PubMed: 19211893]
75. Gusnard DA, Raichle ME. Searching for a baseline: Functional imaging and the resting human brain. Nat Rev Neurosci. 2001; 2:685–694. [PubMed: 11584306]
76. Fornito A, Yucel M, Patti J, Wood SJ, Pantelis C. Mapping grey matter reductions in schizophrenia: An anatomical likelihood estimation analysis of voxel-based morphometry studies. Schizophr Res. 2009; 108:104–113. [PubMed: 19157788]
77. Fornito A, Yucel M, Wood SJ, Adamson C, Velakoulis D, Saling MM, et al. Surface-based morphometry of the anterior cingulate cortex in first episode schizophrenia. Hum Brain Mapp. 2008; 29:478–489. [PubMed: 17525988]
78. Ellison-Wright I, Bullmore E. Meta-analysis of diffusion tensor imaging studies in schizophrenia. Schizophr Res. 2009; 108:3–10. [PubMed: 19128945]
79. van den Heuvel MP, Stam CJ, Kahn RS, Hulshoff Pol HE. Efficiency of functional brain networks and intellectual performance. J Neurosci. 2009; 29:7619–7624. [PubMed: 19515930]

80. Rushton WAH. Theory of the effects of fibre size in medulated nerve. J Physiol. 1951; 115:101–122. [PubMed: 14889433]
81. Shenton ME, Dickey CC, Frumin M, McCarley RW. A review of MRI findings in schizophrenia. Schizophr Res. 2001; 49:1–52. [PubMed: 11343862]
82. Ardekani BA, Nierenberg J, Hoptman MJ, Javitt DC, Lim KO. MRI study of white matter diffusion anisotropy in schizophrenia. Neuroreport. 2003; 14:2025–2029. [PubMed: 14600491]
83. Kanaan RA, Shergill SS, Barker GJ, Catani M, Ng VW, Howard R, et al. Tract-specific anisotropy measurements in diffusion tensor imaging. Psychiatry Res. 2006; 146:73–82. [PubMed: 16376059]
84. O'Donnell LJ, Westin C-F, Golby AJ. Tract-based morphometry for white matter group analysis. Neuroimage. 2009; 45:832–844. [PubMed: 19154790]
85. Oh JS, Kubicki M, Rosenberger G, Bouix S, Levitt JJ, McCarley RW, et al. Thalmo-frontal white matter alterations in chronic schizophrenia: A quantitative diffusion tractography study. Hum Brain Mapp. 2009; 30:3812–3825. [PubMed: 19449328]
86. Mori S, Crain BJ, Chacko VP, Van Zijl PC. Three-dimensional tracking of axonal projections in the brain by magnetic resonance imaging. Ann Neurol. 1999; 45:265–269. [PubMed: 9989633]
87. Behrens TE, Berg HJ, Jbabdi S, Rushworth MF, Woolrich MW. Probabilistic diffusion tractography with multiple fibre orientations: What can we gain? Neuroimage. 2007; 34:144–155. [PubMed: 17070705]
88. Behrens TE, Woolrich MW, Jenkinson M, Johansen-Berg H, Nunes RG, Clare S, et al. Characterization and propagation of uncertainty in diffusion-weighted MR imaging. Magn Reson Med. 2003; 50:1077–1088. [PubMed: 14587019]
89. Jbabdi S, Woolrich MW, Anderson JLR, Behrens TEJ. A Bayesian framework for global tractography. Neuroimage. 2007; 37:116–129. [PubMed: 17543543]
90. Zalesky A. Diffusion tensor magnetic resonance imaging (DT-MRI) fiber tracking: A shortest paths approach. IEEE Trans Med Imaging. 2008; 27:1458–1471. [PubMed: 18815098]
91. Heinrichs RW, Zakzanis KK. Neurocognitive deficit in schizophrenia: A quantitative review of the evidence. Neuropsychology. 1998; 12:426–445. [PubMed: 9673998]
92. Kanaan R, Barker G, Brammer M, Giampietro V, Shergill S, Woolley J, et al. White matter microstructure in schizophrenia: Effects of disorder, duration and medication. Br J Psychiatry. 2009; 194:236–242. [PubMed: 19252154]
93. Wen W, Sachdev PS, Li JJ, Chen X, Anstey KJ. White matter hyperintensities in the forties: Their prevalence and topography in an epidemiological sample aged 44 – 88. Hum Brain Mapp. 2009; 30:1155–1167. [PubMed: 18465744]
94. Schmidt R, Enzinger C, Ropele S, Schmidt H, Fazekas F. Progression of cerebral white matter lesions; 6-year results of the Austrian Stroke Prevention Study. Lancet. 2003; 361:2046–2048. [PubMed: 12814718]
95. Skudlarski P, Jagannathan K, Anderson K, Stevens MC, Calhoun VD, Skudlarska BA, Pearlson G. Brain connectivity is not only lower but different in schizophrenia: A combined anatomical and functional approach. Biol Psychiatry. 2010; 68:61–69. [PubMed: 20497901]

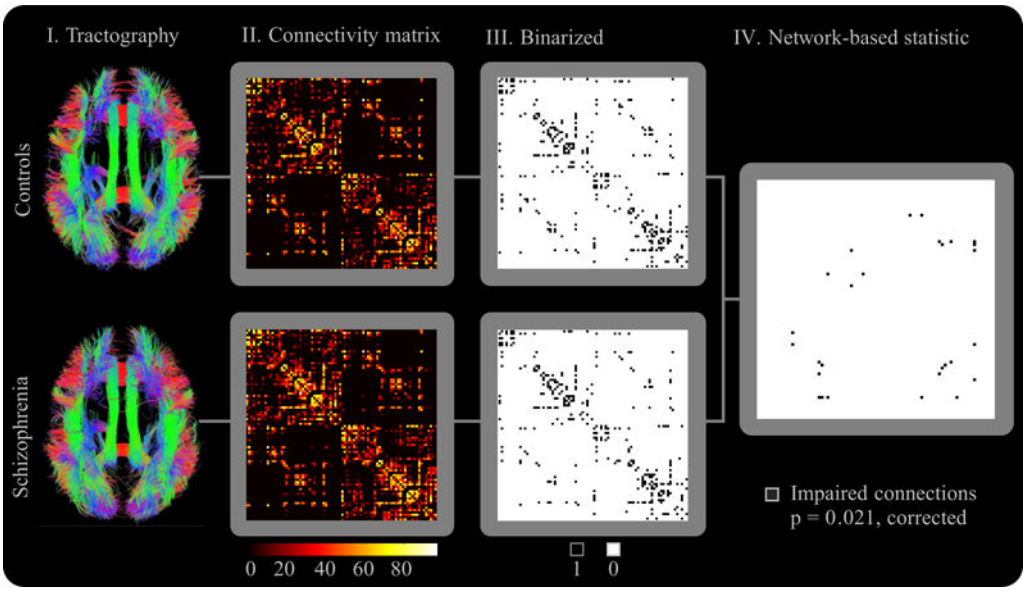

Figure 1.

Overview of methodology. **(I)** The tractographic maps show the set of all cortico-cortical streamlines (normalized to Montreal Neurological Institute space). **II**. Connectivity matrices were populated and **(III)** binarized, where matrix element (*i,j*) quantifies the connectivity (i.e., number of interconnecting streamlines) between node pair (*i,j*). The rows/columns of the connectivity matrix and the binarized connectivity matrix were ordered such that all left hemisphere nodes occupied the first 41 rows/columns. Hence, the two strongly interconnected sub-blocks along the matrix diagonal exclusively involve intrahemispheric connections, whereas the two off-diagonal sub-blocks involve interhemispheric connections. Note the strong contralateral connection profile indicated by the connections along the main diagonal of each interhemispheric sub-block. All matrices represent group averages. **(IV)** The network-based statistic (Methods and Materials) was used to identify impaired connections.

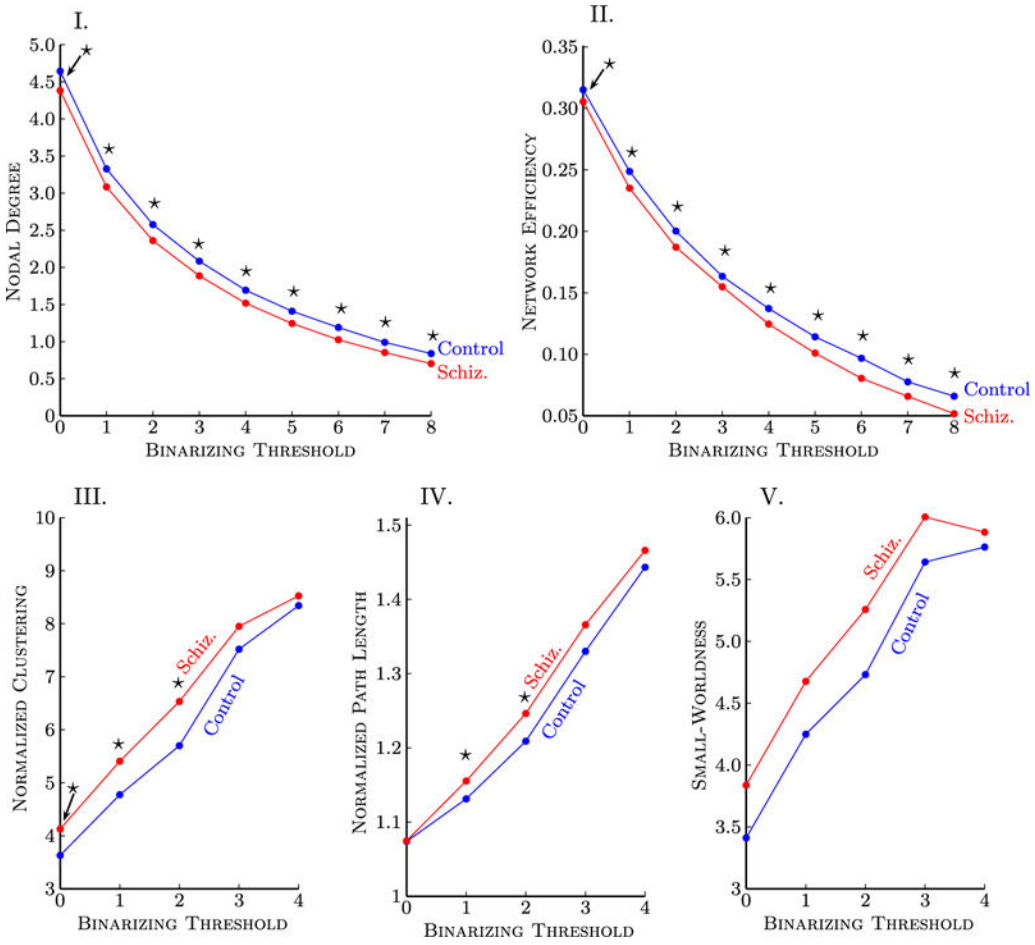

Figure 2.

Graph measures describing topological attributes of corticocortical connectivity were quantified in a sample of patients with schizophrenia. The binarizing threshold (horizontal axis) determined the minimum number of streamlines that needed to interconnect a pair of nodes for a connection to be assumed. Data points marked with a star indicate a significant difference ($p < .05$) between patients and control subjects. Because the same hypothesis was tested at each threshold, correction for multiple comparisons was not performed. Note that $T = 0$ indicates at least one or more streamlines must be present for a link to be drawn. **(I)** Nodal degree and **(II)** network efficiency were reduced in schizophrenia for all binarizing thresholds considered. A trend for increased: **(III)** clustering, **(IV)** path length, and **(V)** small-worldness was demonstrated in patients but was not significant at most thresholds. For binarizing thresholds exceeding $T = 4$, the graph for at least one subject broke apart into two or more disconnected subgraphs. The binarizing threshold was therefore constrained when considering path length, clustering, and small-worldness. The clustering coefficient and path length were normalized with degree-matched random graphs.

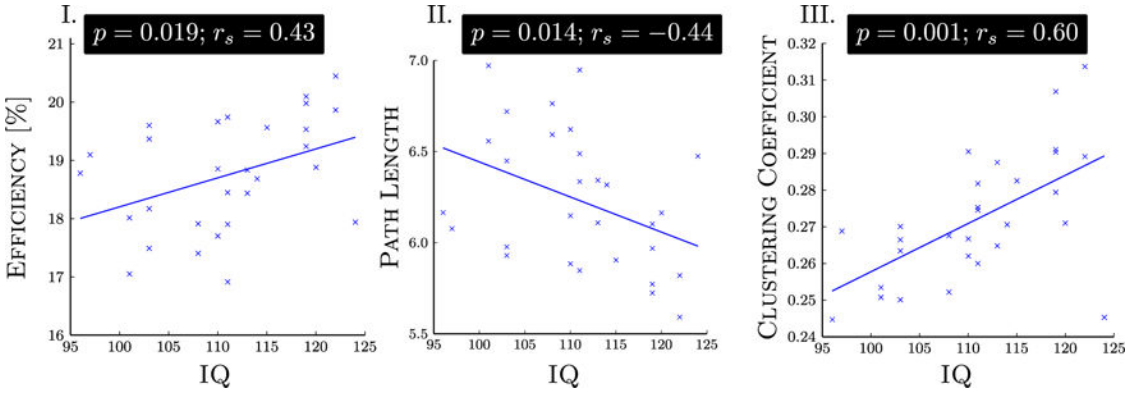

Figure 3.

A linear association was found in the control group between intelligence quotient (IQ), estimated with the Wechsler test of adult reading, and three attributes of network organization: namely, **(I)** global efficiency, **(II)** characteristic path length, and **(III)** average clustering coefficient. No associations with IQ were found in the patient group. Spearman's rank correlation coefficient (r_s) was used to assess the significance of an association. Two control subjects were excluded from this correlation analysis, because IQ data were not available for them.

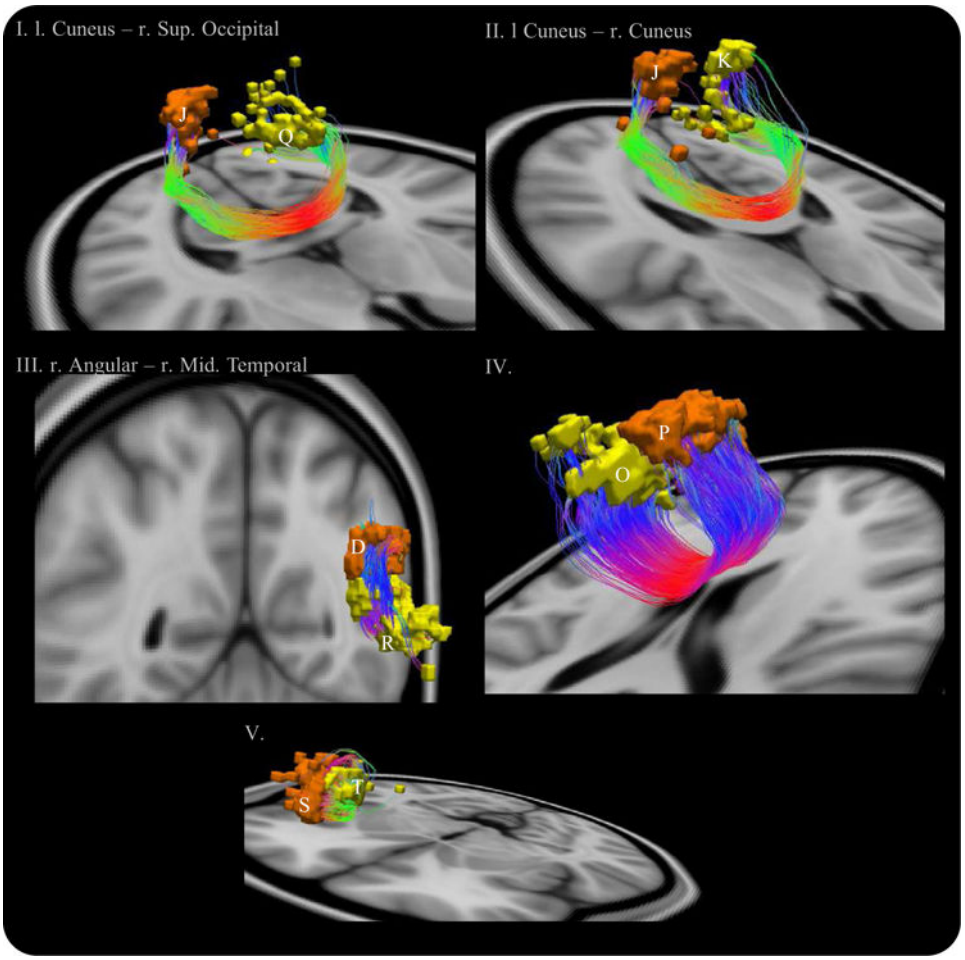

Figure 4.

Impaired connections in patients with schizophrenia satisfying a 10% false discovery rate. Anterior-posterior fibers: green; left–right: red; and superior-inferior: blue. Node abbreviations: (D) right angular; (J) left cuneus; (K) right cuneus; (O) right superior frontal; (P) left superior frontal; (Q) right superior occipital; (R) right middle temporal; (S) left inferior triangularis frontal; and (T) left insula.

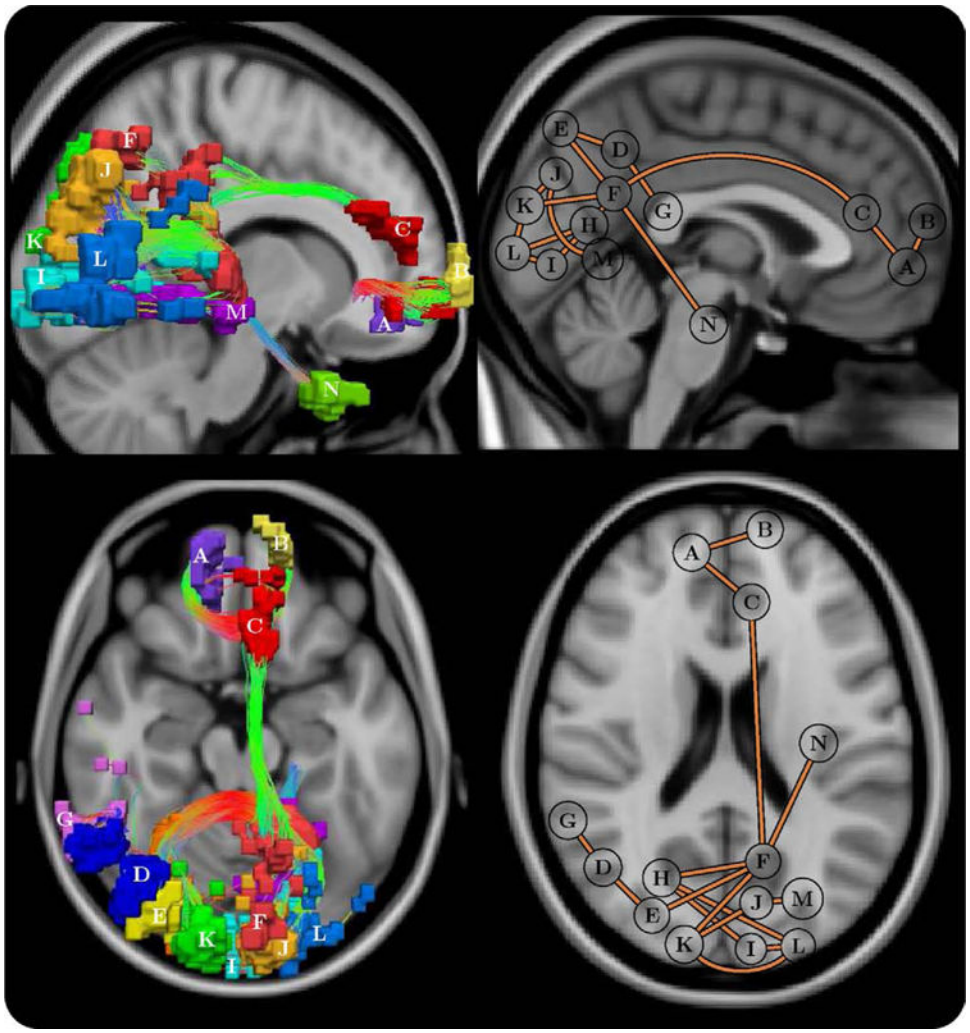

Figure 5.

Schematic of the frontal-parietal/occipital network that was impaired in schizophrenia ($p = .021 \pm .004$, corrected). Each connection comprising this network was impaired in patients but not in control subjects. Left: uniquely colored nodes and streamline representation of interconnecting fiber bundles. Anterior-posterior fibers: green; left–right: red; and superior-inferior: blue. Right: planar graph representation, where each node is depicted as a circle positioned at its node's center of gravity. Note that the positioning of some posterior nodes was slightly shifted from the true center of gravity to avert overlapping. Top: sagittal, left hemisphere. Bottom: axial. Node abbreviations: (A) right medial orbital frontal, (B) left superior medial frontal, (C) left anterior cingulate, (D) right angular, (E) right superior occipital, (F) left precuneus, (G) right superior temporal, (H) right calcarine, (I) left calcarine, (J) left cuneus, (K) right cuneus, (L) left middle occipital, (M) left lingual, and (N) left fusiform.